A Comparison of Atmospheric Quantities Determined from Advanced WVR and Weather Analysis Data

David Morabito,* Longtao Wu,† and Stephen Slobin‡

ABSTRACT. — Lower frequency bands used for deep space communications (e.g., 2.3 GHz and 8.4 GHz) are oversubscribed. Thus, NASA has become interested in using higher frequency bands (e.g., 26 GHz and 32 GHz) for telemetry, making use of the available wider bandwidth. However, these bands are more susceptible to atmospheric degradation. Currently, flight projects tend to be conservative in preparing their communications links by using worst-case or conservative assumptions, which result in nonoptimum data return. We previously explored the use of weather forecasting over different weather condition scenarios to determine more optimal values of atmospheric attenuation and atmospheric noise temperature for use in telecommunications link design. In this article, we present the results of a comparison of meteorological parameters (columnar water vapor and liquid water content) estimated from multifrequency Advanced Water Vapor Radiometer (AWVR) data with those estimated from weather analysis tools (FNL). We find that for the Deep Space Network's Goldstone and Madrid tracking sites, the statistics are in reasonable agreement between the two methods. We can then use the statistics of these quantities based on FNL runs to estimate statistics of atmospheric signal degradation for tracking sites that do not have the benefit of possessing multiyear WVR data sets, such as those of the NASA Near-Earth Network (NEN). The resulting statistics of atmospheric attenuation and atmospheric noise temperature increase can then be used in link budget calculations.

I. Introduction

As lower frequency bands have become oversubscribed during the past several decades, NASA has become interested in utilizing higher frequency bands for telemetry return, making use of the available wider spectrum. However, the higher frequency bands are more susceptible to degradation due to the atmosphere. Currently, flight projects tend to design communications links that make use of worst-case or conservative assumptions, which re-

* Communications Architectures and Research Section.
† Science Data Modeling and Computing Section.
‡ Communications Ground Systems Section.

The research described in this publication was carried out by the Jet Propulsion Laboratory, California Institute of Technology, under a contract with the National Aeronautics and Space Administration.

sult in nonoptimal data return. In recent years, several methods of increasing data volume have been used or studied, such as data rate stepping (as the elevation angle changes during a tracking pass), automatic repeat query (ARQ) techniques, arraying, site diversity, and weather forecasting. Previous work found that forecasting for Deep Space Network (DSN) links "improves both the average data return (between 1 dB and 1.9 dB depending on elevation profile and tracking site) and the reliability of the link (in ideal case to 100 percent)" [1]. A more recent study making use of the University Corporation for Atmospheric Research (UCAR) Weather Research and Forecasting (WRF) tool reinforced the results of previous studies that increased data return could be realized using forecasting techniques [2].

In this article, we make use of weather analysis data (referred to as FNL) to extract estimates of meteorological parameters based on numerous data sets. These data sets consist of various measurements extracted from thousands of surface weather stations, upper air stations, ships, aircraft, and satellites.[1] These data serve as input to various tools used to perform gridded analyses, which can produce the best estimates of the state of the atmosphere as a function of time. They can also serve as initial conditions for various forecast tools such as the WRF [3].

In Section II, we discuss the observations and models used in the analysis. In Section III, we examine the statistics and point-to-point estimates of these parameters of precipitable water vapor (PWV) and liquid water (LW) content from the FNL analyses and from the Advanced Water Vapor Radiometer (AWVR) located at the DSN tracking site in Goldstone, California. In Section IV, we discuss the corresponding comparison for the tracking site in Madrid, Spain. In Section V, we make some concluding remarks as well as providing examples of distributions of atmospheric attenuation derived from FNL and AWVR.

II. The Observational Data and Models

The National Centers for Environmental Prediction (NCEP) final (FNL) analysis data is a global atmospheric analysis data set, which uses observations and NCEP's Global Forecast System (GFS) to produce a representation of the atmospheric state over a regular grid.[2] It provides a multivariate, spatially complete, and coherent record of the global atmospheric circulation. The FNL analysis was run operationally at 12-hr intervals to generate multiple-day weather forecasts over a several-year period. These analyses are produced each time a model completes a forecast cycle. The FNL analyses provide the most complete set of observations available for a given cycle. The FNL from a given cycle (considered the best available analysis) is then applied in the initialization for the next cycle.[3]

FNL data are available on pairs of 1.0 deg "horizontal" hemispheric grids (both north and south) referenced at Earth's surface, 16 vertical levels from 1000 mb up to 10 mb, at the tropopause, at the boundary layer, and some others such as two subsurface levels.[4] The

[1] See website at http://www.cgd.ucar.edu/cas/tn404/text/tn404_9.html#HEADING32-b.

[2] See website at https://rda.ucar.edu/datasets/ds083.0/#!description.

[3] Ibid.

[4] Ibid.

parameters include surface pressure, sea level pressure, geopotential height, temperature, sea surface temperature, potential temperature, relative humidity, snow depth, precipitable water, cloud water content, winds, and vertical motion.[5] The FNL estimates at a particular grid location can be compared to independent estimates derived from data from the AWVR located at the center of that grid location at the same time stamps. The FNL-generated estimates of meteorological profiles are thus referenced for a grid location centered at DSN 34-m-diameter, Ka-band-capable beam-waveguide antennas at Goldstone and Madrid, which were located near the AWVRs during the period of the study.

A favorable comparison would suggest that one could use FNL statistics as inputs to accepted models that yield estimates of atmospheric degradation suitable for input to space–ground link budgets, at sites that do not have the benefit of having statistics derived from years of WVR data. These are used in place of less-accurate statistics such as those derived from global maps of these quantities or based on surface data at the site which serve as input to International Telecommunication Union (ITU) models [4].

WVRs have been in operation at all three DSN tracking sites for several years, providing the data in which to test and quantify the analyses and tool performance. These instruments measure sky brightness temperature over three different frequencies (22.2 GHz, 23.8 GHz, and 31.4 GHz) that reside near the water vapor absorption line at 22.235 GHz. The 31.4-GHz brightness temperature allows for the generation of statistics of atmospheric attenuation and atmosphere noise temperature for the NASA DSN tracking sites. These statistics are made available to flight projects and mission planners in appropriate documentation [5,6]. We have used multifrequency sky brightness temperature measured from the AWVRs to also generate estimates of meteorological parameters of wet path delay, liquid water content, and water vapor content. We use these results for a variety of applications, and their statistics were characterized and reported on previously [7]. In this article, we present comparisons of meteorological parameters obtained from AWVRs with those obtained from the FNL analysis for both Goldstone and Madrid DSN tracking sites. Such a comparison involving FNL data with older-style WVR data for the Canberra DSN tracking site is a focus of future study. Since the Madrid and Canberra climates are similar, the comparison involving Madrid should suffice for this study.

III. Comparison of AWVR- and FNL-Derived Values of Meteorological Parameters for Goldstone

A. Precipitable Water Vapor

Figure 1(a) displays AWVR- and FNL-derived values of PWV from data acquired from 2001 to 2015 (along a vertical column centered at the Goldstone DSN deep space station DSS-25). These two data sets agree reasonably well, showing a generally linear trend (with slope close to unity) and with most points lying between 0 and 4 cm. This diagram is very similar to others found in the literature, such as a comparison of integrated water vapor derived from radiosonde measurements and those retrieved from GPS measurements [8].

[5] Ibid.

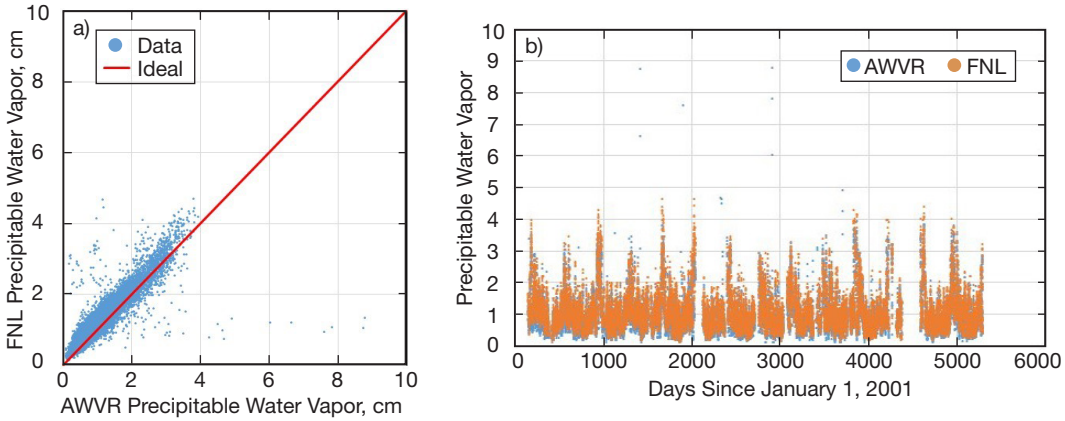

Figure 1. (a) Goldstone precipitable water vapor from AWVR (horizontal axis) and FNL (vertical axis) for years 2001 to 2015; (b) Goldstone precipitable water vapor from AWVR and FNL versus time (number of days since January 1, 2001) for years 2001 to 2015.

From the summary of the statistics shown in Table 1 for both data sets, there is a high degree of correlation (0.91) over the 16981 data points for Goldstone. The average values of the AWVR (1.0 cm) and FNL (1.12 cm) are in reasonable agreement, with the FNL values lying somewhat higher, as seen in Figure 1(a), with more data points lying above the ideal bisecting red line than below it. We believe that this asymmetry may be representative of differences of the AWVR directly probing the vertical cells centered at the DSS-25 tracking station at Goldstone versus the indirect estimation of the effects along this "path" based on the FNL analyses.

Table 1. Summary precipitable water vapor statistics, in centimeters.

	AWVR		FNL			
Site	Mean, cm	Standard Deviation, cm	Mean, cm	Standard Deviation, cm	Correlation Coefficient	Number of Data Points
Goldstone	1.00	0.62	1.12	0.62	0.91	16981
Madrid	1.38	0.61	1.45	0.58	0.90	11965

The time series of the two data sets [Figure 1(b)] overlap reasonably well. There is a small seasonal variation that is evident at the bottom portion of the envelope. Here we see more of the AWVR points (blue) lying somewhat below the FNL values (orange). During the summers, we see high "spikes" near 4 cm. Outside of the summer periods, the high side of the envelope reaches about 2 cm. We can get a closer look at the correlation between the two data sets if we expand the scale to view a single year of data. Figure 2 shows the time series results for year 2013, where the variations between the two data sets track reasonably well.

We can compare the ITU-derived value of the median (1.086 cm) [9] with the medians of the AWVR (0.849 cm) and the FNL (0.976 cm). We see that the FNL median of PWV lies closer to that of the ITU. However, both AWVR and FNL median values lie below those of the ITU. We previously found that some ITU-derived values (such as 0.01 percent rain rate) were overly pessimistic for Goldstone [6]. Using the FNL values in lieu of the AWVR data results in a 15 percent error, whereas using the ITU-R values in lieu of the AWVR data results in a larger 28 percent error. We believe that the AWVR-derived values are more representative of the statistics along the vertical column centered at DSS-25 and the AWVR. The

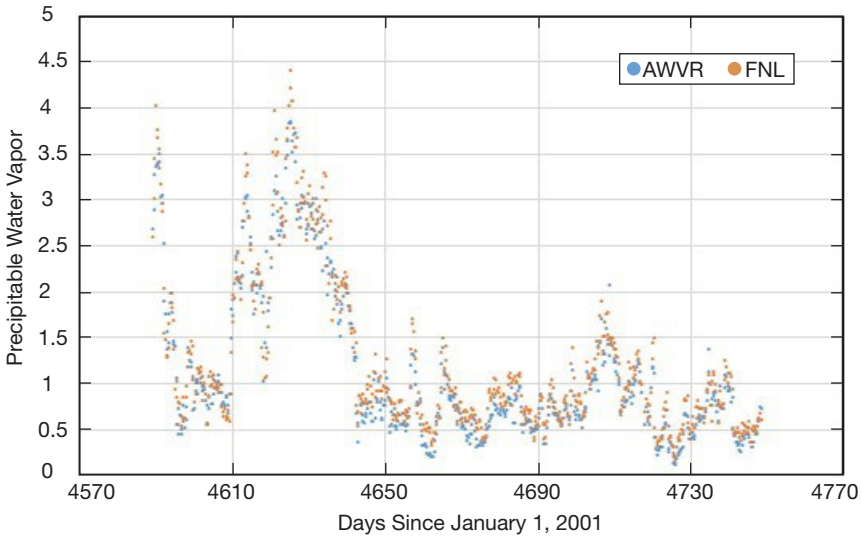

Figure 2. Goldstone precipitable water vapor from AWVR and FNL versus time for year 2013 (versus number of days since January 1, 2001).

statistics using the other two (FNL and ITU) methods are based on "externally" available data whose periods of data usage do not coincide with each other and whose methods (or models) of estimation differ.

B. Cloud Liquid Content

Figure 3(a) displays AWVR and FNL estimates of cloud liquid. Here we do not see the roughly linear relationship that was the case for precipitable water vapor [Figure 1(a)]. However, we do see a roughly symmetric distribution on both sides of the bisecting ideal red line with a somewhat concave shape below ~500 μm. Since cloud liquid is not as well distributed in the atmosphere as water vapor, we would not expect to see the "linear-like" relationship between concurrent estimates, but we do expect the distribution of the two series to be similar or symmetrical about the bisecting ideal line over sufficiently long periods. The liquid water content from the AWVR was derived from sky brightness temperature measurements probing a vertical path centered at the AWVR. The FNL estimates make use of the liquid content distribution in the sky estimated by the FNL analysis carried over the vertical column (centered at the site) by the FNL wind estimates.

Figure 3(b) displays the time series of cloud liquid content for both AWVR and FNL, where both data sets show high correlation in time. Figure 4 displays the cloud liquid comparison for a single year (2003) to allow for better visualization on an expanded scale. Figure 5 displays the cumulative distributions (CDs) of the cloud liquid estimates extracted from AWVR data and FNL data. We see that the distributions are similar where both curves appear to intersect the vertical axis near ~60 percent, consistent with the fact that most of the time there is little or no cloud liquid present in the desert environment of Goldstone. The FNL curve in Figure 5 shows a somewhat higher liquid content than that of the AWVR for a given CD. For instance, at 90 percent, the FNL value of cloud liquid is 38.7 μm and for the AWVR it is 22.1 μm.

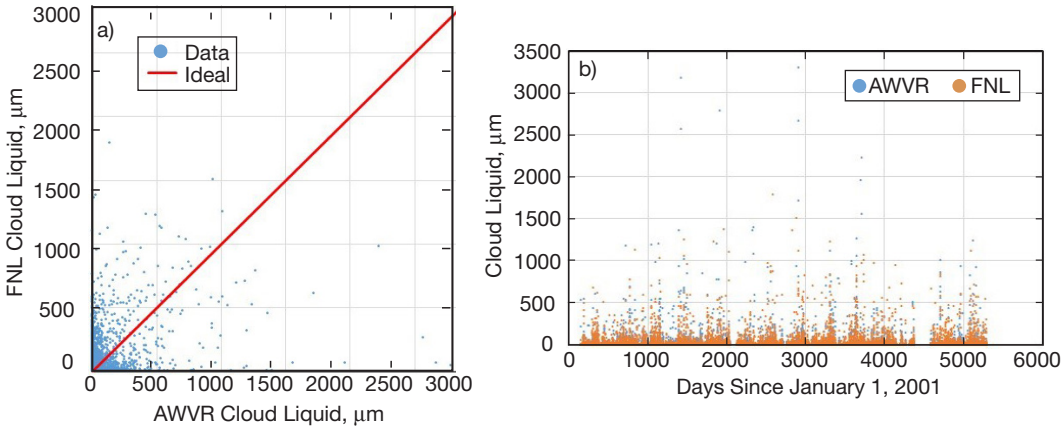

Figure 3. (a) Goldstone cloud liquid content for AWVR (horizontal axis) and FNL (vertical axis); (b) Goldstone cloud liquid content for AWVR and FNL versus time for 2001 to 2015.

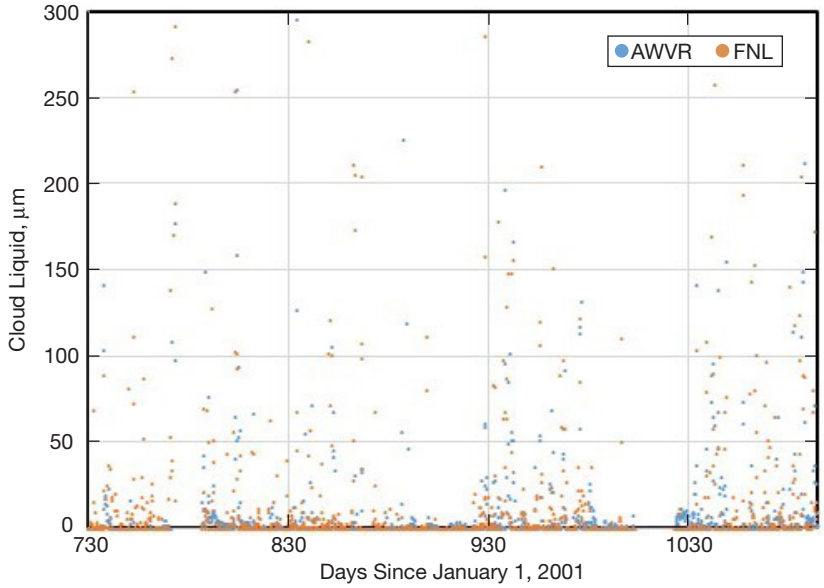

Figure 4. Goldstone cloud liquid content for AWVR and FNL versus time for 2003.

IV. Comparison of AWVR- and FNL-Derived Values of Meteorological Parameters for Madrid

A. Precipitable Water Vapor

Figure 6(a) displays AWVR- and FNL-derived values of PWV along a column centered on DSN station DSS-54 for Madrid, showing a generally linear trend (with slope close to unity) with most data points lying between 0 and 3.6 cm. From the summary of the statistics shown in Table 1, we see a high degree of correlation (0.90) over the 11965 data points covering data from years 2006 to 2015, with somewhat higher FNL values (more points lie above the bisecting ideal curve). The average values of the AWVR and FNL data lie reasonably close to each other. Figure 6(b) displays the time series for the two data sets. We see a

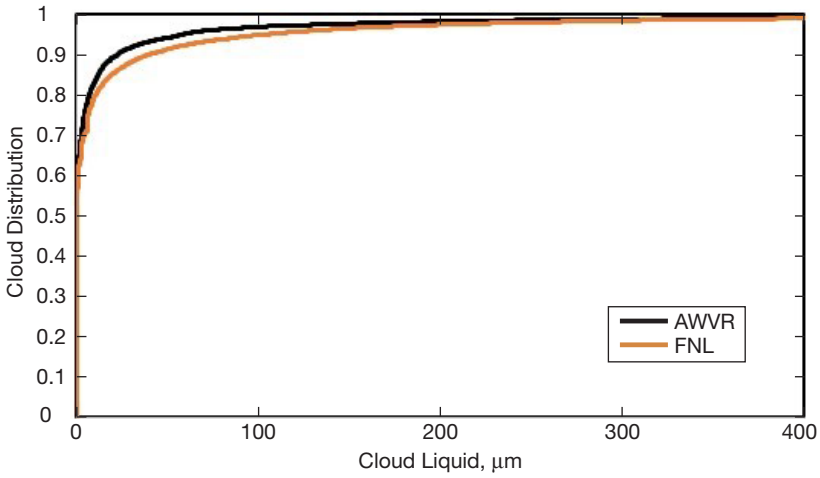

Figure 5. Cumulative distribution curves of cloud liquid for Goldstone.

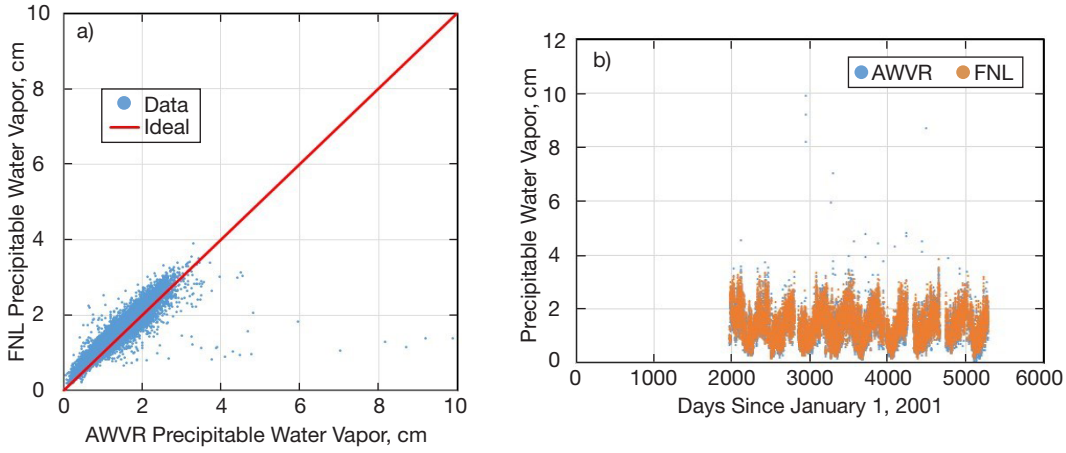

Figure 6. (a) Madrid precipitable water vapor from AWVR (horizontal axis) and FNL (vertical axis); (b) Madrid PWV from AWVR and FNL versus time (days since January 1, 2001).

longer enhanced annual variation than what we observed for Goldstone with this variation being evident both at the upper and lower edges of the envelopes. During the summers, we see "spikes" reaching near peaks of 3.5 cm. Outside of these summer periods, the high side of the envelope reaches about 2 cm. We can get a closer look at the correlation between the two data sets if we expand the scale to view a single year of data (see Figure 7 for 2007). Here the variations between the two data sets track reasonably well. We can compare Madrid PWV medians with an ITU-derived value [9]. The medians of the AWVR data (1.33 cm) and the FNL data (1.42 cm) are in reasonable agreement with those of the ITU (1.31 cm) with better agreement seen between the AWVR and ITU.

B. Cloud Liquid Content

We show AWVR and FNL estimates of cloud liquid in Figure 8(a). Here we do not see the roughly linear relationship that was the case for PWV [see Figure 6(a)]. However, we do see that there is a roughly symmetric distribution on both sides of a bisecting linear line with

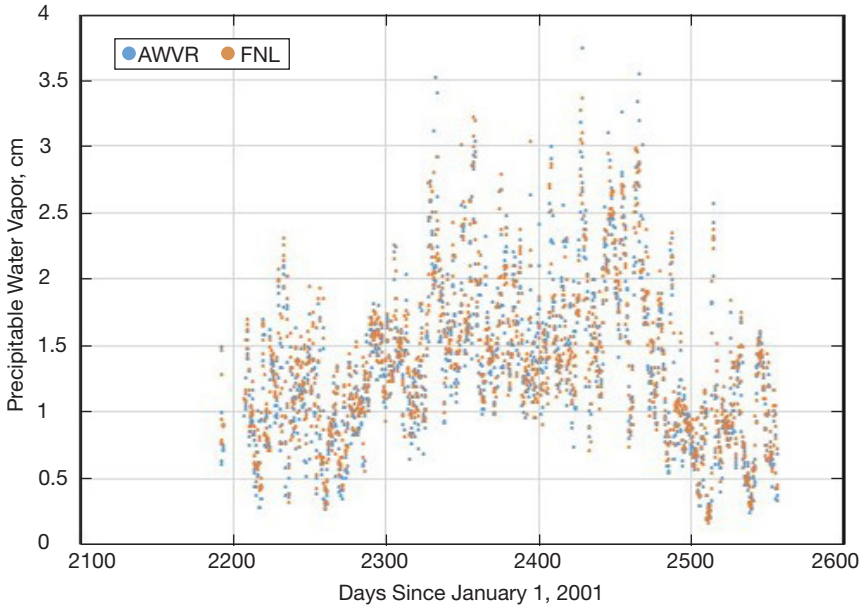

Figure 7. Madrid precipitable water vapor from AWVR and FNL for year 2007 versus number of days since January 1, 2001.

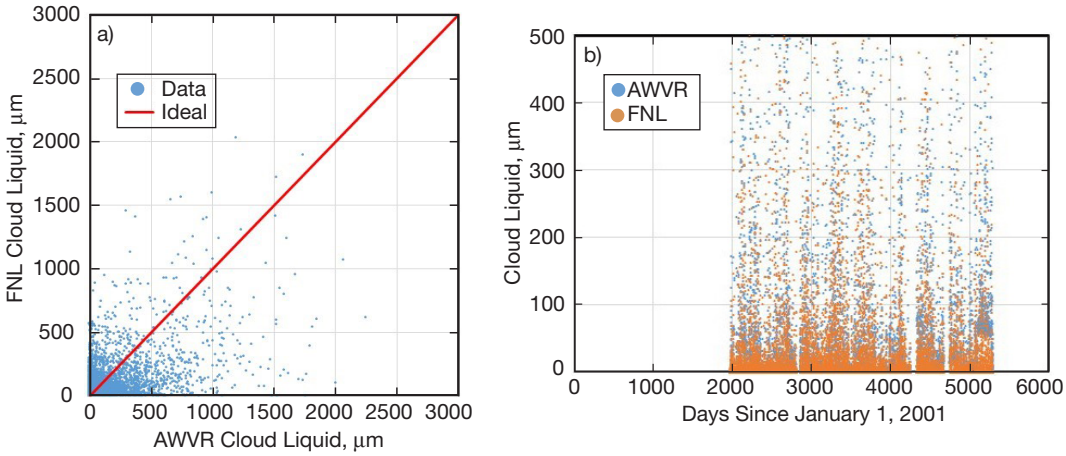

Figure 8. (a) Cloud liquid content for AWVR (horizontal axis) and FNL (vertical axis); (b) cloud liquid content for AWVR and FNL versus time for 2001 to 2015.

most points lying roughly within 500 µm of the origin. Although it does not show the more evident "concave-like" shape below 500 µm (as was the case for Goldstone), the Madrid cloud liquid appears to be reasonably distributed symmetrically along the line bisecting between AWVR and FNL estimates, where there are a slightly higher number of points lying above 500 µm for the AWVR.

Figure 8(b) displays the time series of cloud liquid content for both AWVR and FNL. Given that Madrid is wetter than Goldstone, we do see correlations of the two data sets being consistent between wetter periods and drier periods. Figure 9 displays the cumulative distributions of the cloud liquid estimates extracted from the AWVR and FNL data sets. The distributions are similar where both curves appear to intersect the vertical axis near ~30 percent

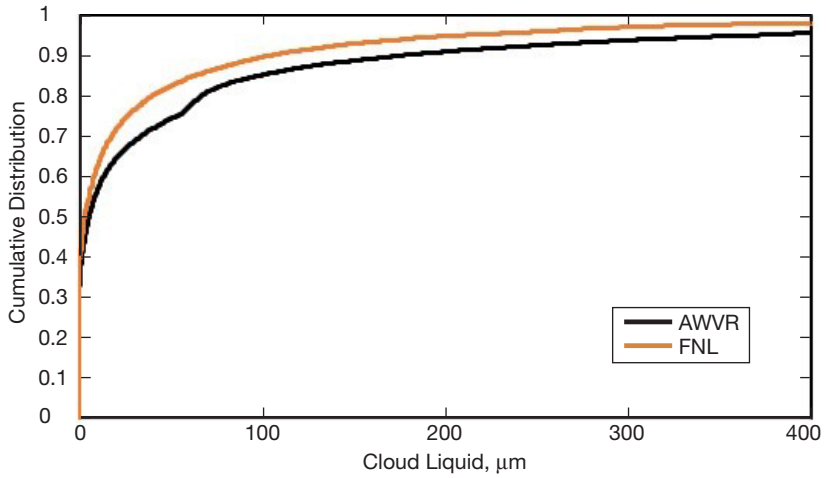

Figure 9. Cumulative distribution curves of cloud liquid for Madrid.

CD, consistent with the fact that there is more cloud liquid present for the Madrid climate over longer periods than for Goldstone. The AWVR distribution curve in Figure 9 shows a higher liquid content than that of the FNL for a given percentile, whereas for Goldstone (see Figure 5) the opposite was true.

V. Concluding Remarks

The statistical consistency of the AWVR and FNL estimates of meteorological parameters provides a degree of confidence in using weather data analysis tools to generate statistics of meteorological parameters. The implication of this study is that statistics of integrated water vapor (PWV) and columnar liquid content (LW) based on FNL analysis data can be used to generate statistics of atmospheric effects for use in telecommunications link budgets for sites that do not have the benefit of years of WVR measurements. The PWV and LW statistics can then be used in place of or in conjunction with ITU-R–derived statistics of these quantities (using ITU or other models).

We can use weather analysis tools to generate multiple-layer estimates of meteorological parameters over sufficiently long periods, which yield zenith estimates of sky temperature at the appropriate link frequency using techniques similar to those presented in [2]. The zenith sky temperature estimates can be converted to values of atmospheric noise temperature and atmospheric attenuation using appropriate formulation. We can then generate the statistics for input to link calculations.

For a test, we applied a basic model to translate the FNL statistics to those of zenith atmospheric attenuation at 31.4 GHz and compared them with those extracted from 31.4 GHz AWVR sky temperature measurements. The CDs are plotted in Figure 10(a) for Goldstone and Figure 10(b) for Madrid. The CD values for the FNL data were derived using basic preexisting coefficients for oxygen, water vapor, and liquid water (labeled as “FNL Original”). The “FNL Fitted” curves in Figures 10(a) and 10(b) result from modifying the standard absorption coefficients for gaseous oxygen, water vapor, and liquid water [10] to provide a best-fit

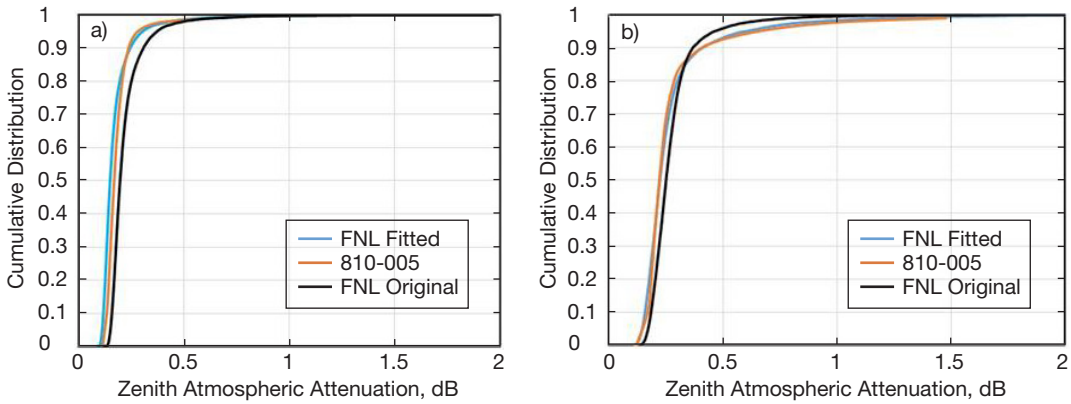

Figure 10. (a) Cumulative distribution of Goldstone 31.4-GHz atmospheric attenuation from FNL with original coefficients (black), FNL with fitted coefficients (blue), and 810-005 [5] at 32 GHz (orange); (b) cumulative distribution of Madrid 31.4-GHz atmospheric attenuation from FNL with original coefficients (black), FNL with fitted coefficients (blue), and 810-005 [5] at 32 GHz (orange).

to the AWVR measurements over the time span of the data sets. We also compared these with values referenced to 32 GHz[6] as obtained from the *DSN Telecommunications Link Design Handbook* [5].

We see from the Goldstone cumulative distributions displayed in Figure 10(a) that atmospheric attenuation estimated with the fit coefficients are in better agreement with those estimated from [5]. The Goldstone atmospheric attenuation CD curves using the "FNL Original" coefficients lie farther to the right. The "FNL Fitted" coefficients have yet to be validated using theory and/or other independent measurements, but are subjects for further study. In any event, the results of Figure 10(a) provide insight into the potential discrepancies for a dry climate.

For Madrid, we see from the cumulative distributions displayed in Figure 10(b) that atmospheric attenuation estimated with the "FNL Fitted" coefficients are in good agreement with those estimated from [5]. The atmospheric attenuation CD curves using the original coefficients agree well with the other two curves for percentiles lying below ~0.9, but diverge somewhat for percentiles above 90 percent. This is not surprising, as the highest percentile data points are dominated by liquid content, which exhibits more dispersion in its atmospheric distribution given Madrid's wetter climate. The new coefficients have yet to be validated from theory or other independent measurements, and are subjects of further study. The results of Figure 10(b) provide some insight for a Madrid-type wet climate.

In order to make use of FNL-generated statistics for non-DSN tracking sites that do not have the benefit of multiyear WVR data sets, we need to validate the available coefficients independently to allow for improved statistics. Future studies would involve comparison tests to be performed on subsets of Goldstone and Madrid data in order to test the "robustness"

[6] For this exercise, we neglect the ~0.3 to 1 K frequency-dependent correction from 31.4 GHz to 32.0 GHz.

of any utilized coefficients. In practice, this approach is not really necessary as one would likely implement a rigorous conversion from PWV and LW to atmospheric attenuation and noise temperature increase using appropriate formulation such as the multilayer atmosphere approach described in [2]. Alternatively, one could use ITU-R models [4] to derive statistics of atmospheric attenuation and noise temperature such as from integrated water content [9].

The level of agreement between AWVR-derived and FNL-derived values of integrated water vapor and liquid water presented in this article provides a degree of confidence using FNL data analysis to generate statistics of these quantities for non-WVR sites.

Acknowledgments

We thank Steve Keihm for generating the AWVR data sets used in this comparison study; B. Geldzahler, F. Davarian, S. Townes, and K. Cheung for support of this work; and Peter Kinman for his thorough review of this article.

References

[1] S. Shambayati, "On the Benefits of Short-Term Weather Forecasting for Ka-band (32 GHz)," *Proceedings, IEEE Aerospace Conference, Volume 3*, pp. 1498, 2004. http://dx.doi.org/10.1109/AERO.2004.1367924

[2] D. Morabito, L. Wu, and S. Slobin, "Weather Forecasting for Ka-band Operations: Initial Study Results," *The Interplanetary Network Progress Report*, vol. 42-206, Jet Propulsion Laboratory, Pasadena, California, pp. 1–24, August 15, 2016. http://ipnpr.jpl.nasa.gov/progress_report/42-206/206C.pdf

[3] W. C. Skamarock, J. B. Klemp, J. Dudhia, D. O. Gill, D. M. Barker, W. Wang, and J. G. Powers, *A Description of the Advanced Research WRF Version 3*, NCAR Technical Note TN-468+STR, 113 pp, 2008.

[4] International Telecommunication Union, "Method for Calculating Link Performance in the Space Research Service," Recommendation ITU-R SA.2183, Electronic Publication, Geneva, Switzerland, October 2010.

[5] S. D. Slobin, "Atmospheric and Environmental Effects," *DSN Telecommunications Link Design Handbook*, DSN No. 810-005, Space Link Interfaces, Module 105, Rev. E, Jet Propulsion Laboratory, Pasadena, California, October 22, 2015 (2015A). http://deepspace.jpl.nasa.gov/dsndocs/810-005/105/105E.pdf

[6] D. D. Morabito, "A Comparison of Estimates of Atmospheric Effects on Signal Propagation Using ITU Models: Initial Study Results," *The Interplanetary Network Progress Report*, vol. 42-199, Jet Propulsion Laboratory, Pasadena, California, pp. 1–24, November 15, 2014. http://ipnpr.jpl.nasa.gov/progress_report/42-199/199D.pdf

[7] D. D. Morabito, S. Keihm, and S. Slobin, "A Statistical Comparison of Meteorological Data Types Derived from Deep Space Network Water Vapor Radiometers," *The Interplanetary Network Progress Report*, vol. 42-203, Jet Propulsion Laboratory, Pasadena, California, pp. 1–21, November 15, 2015.
http://ipnpr.jpl.nasa.gov/progress_report/42-203/203A.pdf

[8] C. R. Ruckstuhl, J. Philipona, J. Morland, and A. Ohmura, "Observed Relationship Between Surface Specific Humidity, Integrated Water Vapor, and Longwave Downward Radiation at Different Altitudes," *Journal of Geophysical Research*, vol. 112, D03302, 2007.
doi:10.1029/2006JD007850

[9] International Telecommunication Union, "Water Vapour: Surface Density and Total Columnar Content," Recommendation ITU-R P.836-3, Electronic Publication, Geneva, Switzerland, November 2001.

[10] Fawwaz T. Ulaby, et al., *Microwave Remote Sensing — Active and Passive — Volume 1 — Microwave Remote Sensing Fundamentals and Radiometry*, Reading, Massachusetts: Addison-Wesley Publishing Company, 1981.